ACES Asian Chemical Editorial Society

doi.org/10.1002/asia.202201203

CHEMISTRY AN ASIAN JOURNAL Research Article

www.chemasianj.org

Special Collection

Solid-state NMR Spectroscopy of Iodine(I) Complexes

Jas S. Ward,* Elina I. Sievänen, and Kari Rissanen*[a]

Abstract: Solid-state NMR has been applied to a series of Barluenga-type iodine(I) [**L**-I-**L**]PF_6 (**L** = pyridine, 4-ethylpyridine, 4-dimethylaminopyridine, isoquinoline) complexes as their hexafluorophosphate salts, as well as their respective non-liquid ligands (**L**), their precursor silver(I) complexes, and the respective N-methylated pyridinium and quinolinium hexafluorophoshate salts. These results are compared and contrasted to the corresponding solution studies and single-crystal X-ray structures. As the first study of its kind on the solid-state NMR behavior of halogen(I) complexes, practical considerations are also discussed to encourage wider utilization of this technique in the future.

Introduction

Halogen(I) ions (also known as *halenium* ions)[1] are the ultimate state of halogen atoms that have been fully ionized to a formally positive ion, X^+ (X = Cl, Br, I), and when stabilized by a pair of Lewis bases (**L**) form Barluenga-type iodine(I) [**L**-X-**L**]$^+$ complexes (*viz. halonium* ions).[2,3] These complexes can be straightforwardly synthesized from their respective silver(I) analogues via Ag^+ to X^+ (X = Br, I) cation exchange (Scheme 1, **a**→**b**) in usually quantitative reactions for a range of Lewis bases, though being predominantly reported with *N*-heterocyclic-based ligands.[2,4] The stability of the complexes is proportional to the size of the halogen atom, such that I > Br > Cl, and this is reflected in the number of examples of each reported in the solid state.[5] Whilst iodine(I) complexes were first structurally characterized in the 1960s,[6–9] they were not popularized until the 1990s when Barluenga and co-workers reported a myriad of invaluable organic transformations using his eponymous reagent, *bis*(pyridine)iodine(I) tetrafluoroborate (*Barluenga's reagent*), [**1**-I-**1**]BF_4, such as the electrophilic iodination of unactivated arenes, the promotion of C–C and C–X bond formation, and the selective direct iodination of peptides.[10–12] More recently, halogen(I) complexes have found utility beyond their intrinsic reactivity as organic reagents, largely owing to the electronic origin (σ-hole)[13] of this type of interaction which strongly enforces a linear geometry, toward the construction of supramolecular architectures.[14–19]

The study of non-covalent interactions has long benefitted from nuclear magnetic resonance (NMR) methods complementing the single crystal X-ray diffraction (SCXRD) results, as in addition to the molecular geometry from the SCXRD, the NMR studies can provide information on the molecular and electronic structures.[20] Important thermodynamic and kinetic data, for example the strengths of interactions or the rate constants of dynamic processes involving non-covalent interactions, can be determined by NMR spectroscopic methods.[21] The NMR spectroscopy in the solid state, *viz.* SS-NMR, has benefits in that it is sensitive to polymorphism and co-crystallization processes,[22] can provide structural information that directly relates to available single crystal diffraction data,[23,24] and can supplement these studies for systems that are disordered or exhibiting internal dynamics.[25,26]

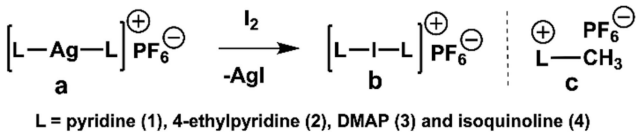

L = pyridine (1), 4-ethylpyridine (2), DMAP (3) and isoquinoline (4)

Scheme 1. The reaction to synthesize iodine(I) complexes from their respective silver(I) analogues via Ag^+ (**a**) to I^+ (**b**) cation exchange. The N-methyl pyridinium salt from ligand **L** (**c**).

The study of traditional halogen bonds of the form R–X···Y (R = substituent, X = halogen, Y = electron donor) have already benefitted from the implementation of solid-state NMR methods (Figure 1),[27,28] given that the halogen bonding interactions of these systems rarely persist in solution due to their relatively weak strength. Earlier studies on two-component, halogen-bonded systems (*e.g.*, tertiary amines with iodo-perfluoroalkanes), found great utility with ^{14}N (and ^{19}F) NMR studies due to the significant shifts experienced by both components upon halogen bonding.[29] Solid-state NMR studies,[30–33] especially ^{15}N,[34–36] have also proven invaluable toward offering real-world applications of halogen bonding, as has been deftly demonstrated for 3-iodo-2-propynyl-*N*-butylcarbamate (IPBC) via a

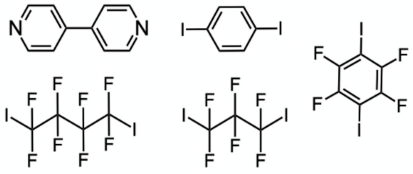

Figure 1. Solid-state ^{15}N NMR spectroscopy has been previously used to observe the halogen-bonded coordination networks that are constructed from the outlined halogen bond acceptor, 4,4′-bipyridine, and a range of halogen bond donors.[27,28]

[a] *Dr. J. S. Ward, Dr. E. I. Sievänen, Prof. K. Rissanen*
University of Jyvaskyla
Department of Chemistry
Jyväskylä 40014 (Finland)
E-mail: james.s.ward@jyu.fi
kari.t.rissanen@jyu.fi

Supporting information for this article is available on the WWW under https://doi.org/10.1002/asia.202201203

This manuscript is part of a special collection on Halogen Bonding.

range of halogen-bonded co-crystals,[37] which due to the deficiencies of handling pure IPBC, provided synthetic alternatives with improved properties.

In recent years, the field of halogen(I) chemistry has seen a myriad of advancements, with the observation of the first structurally chiral,[18] unrestrained heteroleptic,[38] hierarchical,[39] and nucleophilic iodine(I) interaction complexes being reported in the solid state.[40–42] This progress had led to a recent infusion of liquid state ^{1}H and ^{15}N NMR data, however, it has also revealed dynamic behavior, such as ligand scrambling, especially for unrestrained heteroleptic halogen(I) complexes.[38,43] The high reactivity of halogen(I) complexes, particularly in solution, has also played a role in limiting the NMR data available in the literature.[4] As a consequence, the field of halogen(I) chemistry is comprised of an abundance of solid-state X-ray structural data, which would benefit from the ability to directly compare NMR spectroscopic results recorded in the same state, obviating any of the solid *vs.* solution state differences that arise, and therefore highlighting any additional information that might have otherwise remained unobserved. As the size, reactivity and/or complexity of halogen(I) complexes increases, for example with the recent report of an iodine(I) halogen-bonded organic framework (XOF) that was for all intents and purposes insoluble,[19] solution NMR studies will become more difficult to obtain. In response, and due to the aforementioned success with traditional halogen-bonded systems, the solid-state NMR spectroscopy on halogen(I) complexes was explored.

Experimental

All reagents and solvents were obtained from commercial suppliers and used without further purification, and all silver(I) and iodine(I) complexes were synthesized as previously reported.[38,44,45] For structural NMR assignments in solution, ^{1}H NMR and ^{1}H-^{15}N NMR correlation spectra were recorded on a Bruker Avance III 500 MHz spectrometer at 25 °C in CD_2Cl_2. Chemical shifts are reported on the δ scale in ppm using the residual solvent signal as internal standard (CH_2Cl_2 in CD_2Cl_2: δ_H 5.32), or for ^{1}H-^{15}N NMR spectroscopy, to an external d_3-$MeNO_2$ standard. For the ^{1}H NMR spectroscopy, each resonance was assigned according to the following conventions: chemical shift (δ) measured in ppm, observed multiplicity, observed coupling constant (*J* Hz), and number of hydrogen atoms. Multiplicities are denoted as: s (singlet), d (doublet), t (triplet), m (multiplet), and br (broad). For the ^{1}H-^{15}N HMBC spectroscopy, spectral windows of 4 ppm (^{1}H) and 300 ppm (^{15}N) were used, with 1024 points in the direct dimension and 512 increments used in the indirect dimension, with subsequent peak shape analysis being performed to give the reported ^{15}N NMR chemical shifts.

The ^{15}N CPMAS NMR spectra were recorded at room temperature with a Bruker Avance 400 MHz spectrometer working at 40.55 MHz for ^{15}N. The spectrometer was equipped with a CPMAS probe and 4 mm ZrO_2 rotors were used. The spectral width (SW) was set to 1002.55 ppm and 40 000–100 000 scans, depending on the sample, were collected. The solid samples were spun at rates of 5, 7.5, or 10 kHz. The cross polarization contact time was 5 ms, with a 4 s relaxation delay. The solid-state spectra were referenced to the $C_2H_5{}^{15}NO_2$ of external glycine $\delta(^{15}N) = 36.6$ ppm (from NH_3), that was measured separately. To convert the measured chemical shifts relative to CH_3NO_2 the equation $\delta(^{15}N) = \delta(^{15}N_{measured}) - 381.7$ ppm was used.

The single crystal X-ray data for **4c** was collected at 120 K using an Agilent SuperNova dual wavelength diffractometer with an Atlas detector using mirror-monochromated Cu–Kα (λ = 1.54184 Å) radiation. The program CrysAlisPro[46] was used for the data collection and reduction on the SuperNova diffractometer, and the intensities were absorption corrected using a gaussian face index absorption correction method. All structures were solved by intrinsic phasing (SHELXT)[47] and refined by full-matrix least squares on F^2 using the OLEX2,[48] utilizing the SHELXL-2015 module.[49] Anisotropic displacement parameters were assigned to non-H atoms and isotropic displacement parameters for all H atoms were constrained to multiples of the equivalent displacement parameters of their parent atoms with $U_{iso}(H) = 1.2\ U_{eq}$ (aromatic) or $U_{iso}(H) = 1.5\ U_{eq}$ (alkyl) of their respective parent atoms. The X-ray single crystal data and CCDC number is included in the Supporting Information.

Synthesis of [Me(3)]PF_6 (3c)

Ligand **3** was dissolved in toluene (5 mL) and then CH_3I (248.9 μL, 4 mmol) was added and heated to 65 °C for 3 hours, after which time a white precipitate had formed. The precipitate was collected by filtration and washed with ethyl acetate (12 mL in small portions). The isolated solid was dissolved in H_2O (6 mL) and to it was added a solution of $[NH_4]PF_6$ (211.9 mg, 1.3 mmol) in H_2O (6 mL) to immediately give a white precipitate. After stirring for 20 minutes, the precipitate was collected by filtration and washed with additional H_2O (8 mL). The precipitate was dissolved in dichloromethane (20 mL) and dried over Na_2SO_4. Removed all insoluble material by filtration and all volatiles were removed from the resulting filtrate to leave a white solid. Recovered yield = 85.8 mg (0.30 mmol, 30 %). ^{1}H NMR (500 MHz, CD_2Cl_2) δ 7.86 (d, *J* = 7.6 Hz, 2H), 6.81 (d, *J* = 7.7 Hz, 2H), 3.94 (s, 3H), 3.22 (s, 6H); ^{15}N NMR (500 MHz, CD_2Cl_2) δ −292.7 (NMe_2), −223.8 (py).

The NMR characterization of **4**, **4a**, and **4b** were repeated in CD_2Cl_2 to enable direct comparisons (N.B. the reported chemical shifts were obtained in CD_3CN to improve the solubilities of the complexes).[45]

Isoquinoline (Isoq; 4)

^{1}H NMR (500 MHz, CD_2Cl_2) δ 9.26 (s, 1H), 8.52 (d, *J* = 5.7 Hz, 1H), 7.97 (d, *J* = 8.2 Hz, 1H), 7.83 (d, *J* = 8.3 Hz, 1H), 7.74–7.56 (m, 3H); ^{15}N NMR (500 MHz, CD_2Cl_2) δ −72.5.

[$Ag(4)_2$]PF_6 (4a)

^{1}H NMR (500 MHz, CD_2Cl_2) δ 9.45 (s, 2H), 8.50 (d, *J* = 6.1 Hz, 2H), 8.16 (d, *J* = 8.2 Hz, 2H), 7.99–7.87 (m, 6H), 7.79 (t, *J* = 7.3 Hz, 2H); ^{15}N NMR (500 MHz, CD_2Cl_2) δ −132.0.

[$I(4)_2$]PF_6 (4b)

^{1}H NMR (500 MHz, CD_2Cl_2) δ 9.55 (s, 2H), 8.55 (d, *J* = 6.3 Hz, 2H), 8.23 (d, *J* = 8.2 Hz, 2H), 8.10–8.02 (m, 4H), 7.96 (d, *J* = 6.3 Hz, 2H), 7.91 (t, *J* = 6.8 Hz, 2H); ^{15}N NMR (500 MHz, CD_2Cl_2) δ −181.6.

Synthesis of [Me(4)]PF_6 (4c)

Ligand **4** was dissolved in toluene (5 mL) and then CH_3I (248.9 μL, 4 mmol) was added and heated to 65 °C for 3 hours, after which time a white precipitate had formed. The precipitate was collected

by filtration and washed with ethyl acetate (12 mL in small portions). The isolated solid was dissolved in H_2O (6 mL) and to it was added a solution of $[NH_4]PF_6$ (211.9 mg, 1.3 mmol) in H_2O (6 mL) to immediately give a pale-yellow precipitate. After stirring for 20 minutes, the precipitate was collected by filtration and washed with additional H_2O (8 mL). The precipitate was dissolved in dichloromethane (20 mL) and dried over Na_2SO_4. Removed all insoluble material by filtration and all volatiles were removed from the resulting filtrate to leave a pale-yellow solid. Recovered yield = 71.5 mg (0.25 mmol, 25%). ^{1}H NMR (500 MHz, CD_2Cl_2) δ 9.57 (s, 1H), 8.44 (d, J = 8.3 Hz, 1H), 8.29 (dd, J = 22.3, 6.5 Hz, 2H), 8.25–8.15 (m, 2H), 8.05 (t, J = 6.9 Hz, 1H), 4.56 (s, 3H); ^{15}N NMR (500 MHz, CD_2Cl_2) δ -189.0. Crystals suitable for single crystal X-ray diffraction were obtained by evaporation of a dichloromethane solution of **4c**. Crystal data for **4c**: CCDC-2178008.

Results and Discussion

The known silver(I), [**L**-Ag-**L**]PF_6 (**1a**–**4a**), and iodine(I) complexes, [**L**-I-**L**]PF_6 (**1b**–**4b**), and two N-methyl ammonium salts (**3c** and **4c**) of four different ligands (L = **1**–**4**) were synthesized for this study (Figure 2). The silver(I) salts could be prepared quantitively by simple addition of two equivalents of the respective ligand to $AgPF_6$. The iodine(I) complexes were prepared by Ag^+ to I^+ cation exchange by reacting the silver(I) salts with a stoichiometric amount of elemental iodine, which is a reliable methodology that has been used to prepare a large range of halogen(I) motifs,[3,14,15] including recently, hypoiodite complexes.[50–52]

The four ligands (**L**) chosen were pyridine (py; **1**), 4-ethylpyridine (4-Etpy; **2**), 4-dimethylaminopyridine (DMAP; **3**), and isoquinoline (isoq; **4**), all of which had previously been reported in the literature.[38,44,45] Ideally only ligands that existed as solids would have been considered to increase the potential breadth of the solid-state studies, though this only offered a small choice of straightforward sample systems in the literature (DMAP and isoq), and therefore other common ligands in the field of halogen(I) chemistry were also included (py and 4-Etpy). The solution data had been reported for all these species, fortuitously in the same solvent (CD_2Cl_2) with the exception of the isoq series (**4**, **4a**, **4b**). Additionally, the N-methyl salts (Scheme 1, **c**) were also synthesized from DMAP (**3c**) and isoq (**4c**). A SS-NMR study of a similar salt, *N*-ethyl isoquinolinium hexafluorophosphate has been reported in the literature.[53]

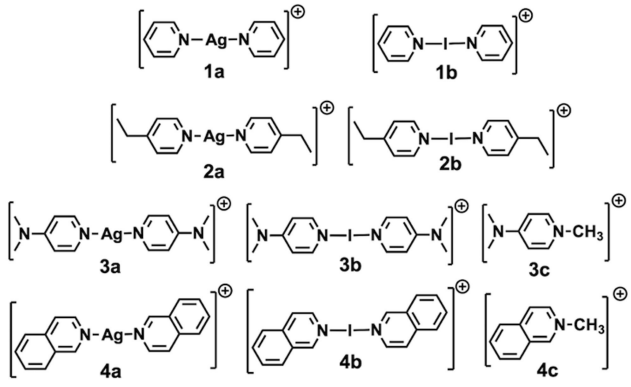

Figure 2. The chemical structures of the studied cationic complexes and their numbering (hexafluorophosphate anions omitted).

The single crystal X-ray structures of the studied silver(I) and iodine(I) complexes **1a**–**4a** and **1b**–**4b** are known and discussed here by referencing their CSD ref codes.[5][1] Complex **1a** is known as the NO_3^- (CSD ref code *AGPYNO*), ClO_4^- (*DITCEO, LULNOX, NEVRAI, KELDAK*), BF_4^- (*LULNIR, NEVREM*), PF_6^- (*LUKZAU, NEVRIQ*), and SbF_6^- (*LUKZIC*) salts; **1b** as the BF_4^- (*HUMMAD*), I_3^- (*PYRIDI*), PF_6^- (*CICQIQ*), SbF_6^- (*LUKZOI*), tosylate (*LULPIF*), NO_3^- (*LULCAY*), ClO_4^- (*DOVYOE, DOVYUK*), and $F_3FSO_3^-$ (*DOVZAR*) salts. Complex **2a** is known as the PF_6^- salt (*SURSUW*), but **2b** is only reported in an exotic co-crystal with *bis*(2,2′-bipyridine)Ag(I) hexafluorophostate (*EPEYUW*). Complex **3a** is known as the NO_3^- (*YUCNIU*), BF_4^- (*IJATOE*), and PF_6^- (*PIZKUF, SURSAC, SURSIK*) salts; **3b** as the NO_3^- (*MIYJIP*) and PF_6^- (*SURTEH*) salts. Complex **4a** is known as the BF_4^- (*RAKPUS*) and PF_6^- (*RAKNEA*) salts; **4b** as the I_3^- (*RAKNIE*), BF_4^- (*RAKQIH*), PF_6^- (*RAKQED*), and $F_3FSO_3^-$ (*RAKQON*) salts. The clamp Ag^+ and I^+ complexes (Figure 4), used here as a reference to the ^{15}N solution studies, are known as their BF_4^- (I, *NUTNUO*, disordered), $F_3FSO_3^-$ (Ag, *APONEE*), PF_6^- (Ag, *NUTPIE*; I, *DAVROL*), and SbF_6^- (*DAVRUR*) salts. Due to the possible anion effect in the SS-NMR, only the X-ray structures of the PF_6^- salts of **1a** (*NEVRIQ*), **1b** (*CICQIQ*), **2a** (*SURSUW*), **3a** (*PIZKUF*), **3b** (*SURTEH*), **4a** (*RAKNEA*), **4b** (*RAKQED*) and **I-clamp** (*DAVROL*) are taken into consideration.

The solid-state ^{15}N NMR spectra of all species were collected as previously stated (*vide supra*; Figure 3) and the results are summarized in Table 1. When compared the resonance line widths of the ^{15}N chemical shifts in the CPMAS spectra ($\Delta\nu_{1/2}$ ~100 Hz for NMe_2 and $\Delta\nu_{1/2} \geq 200$ Hz for N(py), respectively) with those extracted from the liquid state ^{1}H,^{15}N HMBC spectra (*cf.* $\Delta\nu_{1/2}$ ~70–150 Hz for N(py)/NMe_2, depending on the concentration and duration of the HMBC experiment), a remarkable difference is observed. This is due to the incomplete averaging of anisotropic effects by magic angle spinning that leads to line broadening in the observed resonances of the

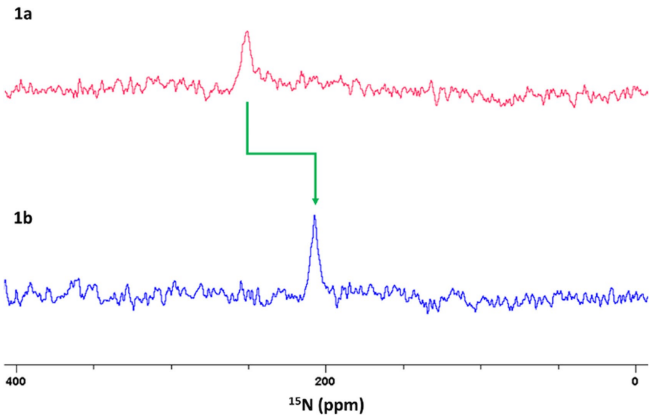

Figure 3. The solid-state ^{15}N NMR spectra of **1a** and **1b** (referenced to zwitterionic form of glycine, $C_2H_5{}^{15}NO_2$), with the characteristic δ_N coordination shift to upfield resulting from the Ag^+ to I^+ cation exchange annotated with a green arrow.

[1] CSD Version 2022.3 (Build 364734).

Table 1. The solid-state ^{15}N NMR chemical shifts for the all complexes studied in this work, and their comparisons to ^{1}H-^{15}N HMBC determined liquid-state ^{15}N NMR chemicals shifts in CD_2Cl_2 (all values in ppm).

Complex	Solid-state δ_N (referenced to $C_2H_5{}^{15}NO_2$)	Solid-state δ_N (adjusted to CD_3NO_2 referencing)	Solution state δ_N (referenced to CD_3NO_2)
Pyridine (**1**)	Liquid (m.p. −42 °C)	Liquid (m.p. −42 °C)	−66.3[38]
$[Ag(py)_2]PF_6$ (**1a**)	252.2	−129.5	−121.6[38]
$[I(py)_2]PF_6$ (**1b**)	207.5	−174.2	−174.8[38]
4-ethylpyridine (**2**)	Liquid (m.p. −91 °C)	Liquid (m.p. −91 °C)	−75.6[38]
$[Ag(4\text{-}Etpy)_2]PF_6$ (**2a**)	251.2	−130.5	−118.6[38]
$[I(4\text{-}Etpy)_2]PF_6$ (**2b**)	199.2	−182.5	−181.9[38]
DMAP (**3**)	61.1 (NMe_2), 276.7 (py)	−320.6 (NMe_2), −109.0 (py)	−328.7 (NMe_2), −108.9 (py)[38]
$[Ag(DMAP)_2]PF_6$ (**3a**)	72.5 (NMe_2), 216.1 (py)	−309.2 (NMe_2), −165.6 (py)	−314.4 (NMe_2), −168.7 (py)[38]
$[I(DMAP)_2]PF_6$ (**3b**)	75.4 (NMe_2), 172.9 (py)	−306.3 (NMe_2), −208.9 (py)	−307.1 (NMe_2), −216.1 (py)[38]
$[Me(DMAP)]PF_6$ (**3c**)	87.1 (NMe_2), 155.3 (py)	−294.6 (NMe_2), −226.4 (py)	−292.7 (NMe_2), −223.8 (py)
Isoquinoline (**4**)	No signal observed (m.p. 26–28 °C)	No signal observed (m.p. 26–28 °C)	−72.5 (−70.1[#])[45]
$[Ag(isoq)_2]PF_6$ (**4a**)	245.0	−136.7	−132.0 (−106.1[#])[45]
$[I(isoq)_2]PF_6$ (**4b**)	201.6	−180.1	−181.6 (−181.9[#])[45]
$[Me(isoq)]PF_6$ (**4c**)	194.3	−187.4	−189.0

[#] Original reported ^{15}N NMR chemical shifts (recorded in CD_3CN).

solid-state spectra – particularly for moderate magnetic field strengths applied and sample spinning speeds.

The observed values revealed remarkable consistency in the chemical shifts of the (adjusted) solid-state values and those recorded in CD_2Cl_2, with differences in the two sets of values within the range of 0.1–11.9 ppm for the pyridyl nitrogen atoms, and for the DMAP species that also included a second nitrogen environment (NMe_2: **3**–**3c**), a difference range of 0.8–8.1 ppm was found. The species with the smallest and largest difference upon comparison for the pyridinic nitrogen atom shifts were **3** (0.1 ppm) and **2a** (11.9 ppm). The smallest difference for the NMe_2 groups was observed for **3b** (0.8 ppm), with **3** (8.1 ppm) demonstrating the largest difference. It should be noted that the iodine(I) complexes (**1b**–**4b**) generally demonstrated the best agreement to their solution-state spectra in CD_2Cl_2, which might be an indication of the more consistent solid-state packing of the iodine(I) complexes, due to the I^+ centers of these complexes usually eschewing intermolecular interactions. This range of differences in **3** between the solution and solid-state data, whereupon the pyridinic nitrogen almost perfect matches and the NMe_2 group has the largest difference observed for this substituent, highlights that these variabilities are real and not dependent on the spectra being compared. The literature values of **4**–**4b** (parenthetically included in Table 1) were reported in CD_3CN due to the poor solubility of **4b** in CD_2Cl_2, which serendipitously highlighted another advantage of solid-state NMR spectroscopy. The progression of free ligand to silver(I) complex, then finally to a halogen(I) complex are often monitored by NMR spectroscopy to follow the electronic changes during the reaction. However, the CD_3CN chemical shift of **4a** (−106.1 ppm) is markedly different from the chemical shift in CD_2Cl_2 (−132.0 ppm), which can be attributed to the opportunistic coordination of CD_3CN to the silver(I) center, something that the CD_2Cl_2 solvent was incapable of. The solid-state determined chemical shift of −136.7 ppm, which corroborates to the CD_2Cl_2 value, removes any ambiguity as to whether the solvent is interacting, and as a result perturbing the observed chemical shift. It should also be noted that in the solid-state ^{15}N NMR spectrum of **3c** the peaks were observed as apparent 'doublets', potentially indicating the presence of multiple polymorphs being present for this complex, which is structural information that could not be obtained by SCXRD as no solid-state structures are currently known for **3c**.

Previous solution based NMR studies by Erdélyi and co-workers on a range of bidentate *bis*(pyridyl)ligand systems (*e.g.*, **I–Clamp**; Figure 4) have been performed to help identify the symmetry of the halogen bonding in $[N{-}X{-}N]^+$ (X = Br, I) halogen(I) complexes.[3,54] These studies indicated that halogen(I) ions existed as symmetrical complexes, rather than the possible alternative of asymmetrical ligand-stabilized halopyridinium, $[N{-}X{\cdots}N]^+$, complexes. The bulk of SCXRD data of $[N{-}X{-}N]^+$ complexes supports the symmetrical nature of the halogen bonding (once the esds of the SCXRD measurements are taken into account), however, the fluxional nature of recently reported heteroleptic iodine(I) complexes is not suited to solution NMR studies due to the ligand scrambling they are susceptible to.[38,43] Therefore, this represents a niche area where the development of SS-NMR methodologies could provide results.

Despite the clear variation of the ^{15}N NMR chemical shifts between the studied silver(I) and iodine(I) complexes (Table 1) both in the solution and in the solid state, the X-ray structures of them do not show such variation. The Ag–N and I–N bond distances and the N–I–N angles (Figure 4) are remarkably constant, fitting very well with the average values of a large set of similar iodine(I) complexes.[55] The very small N–I–N asymmetry observed in the X-ray structure the **I-clamp** (Figure 4) is not

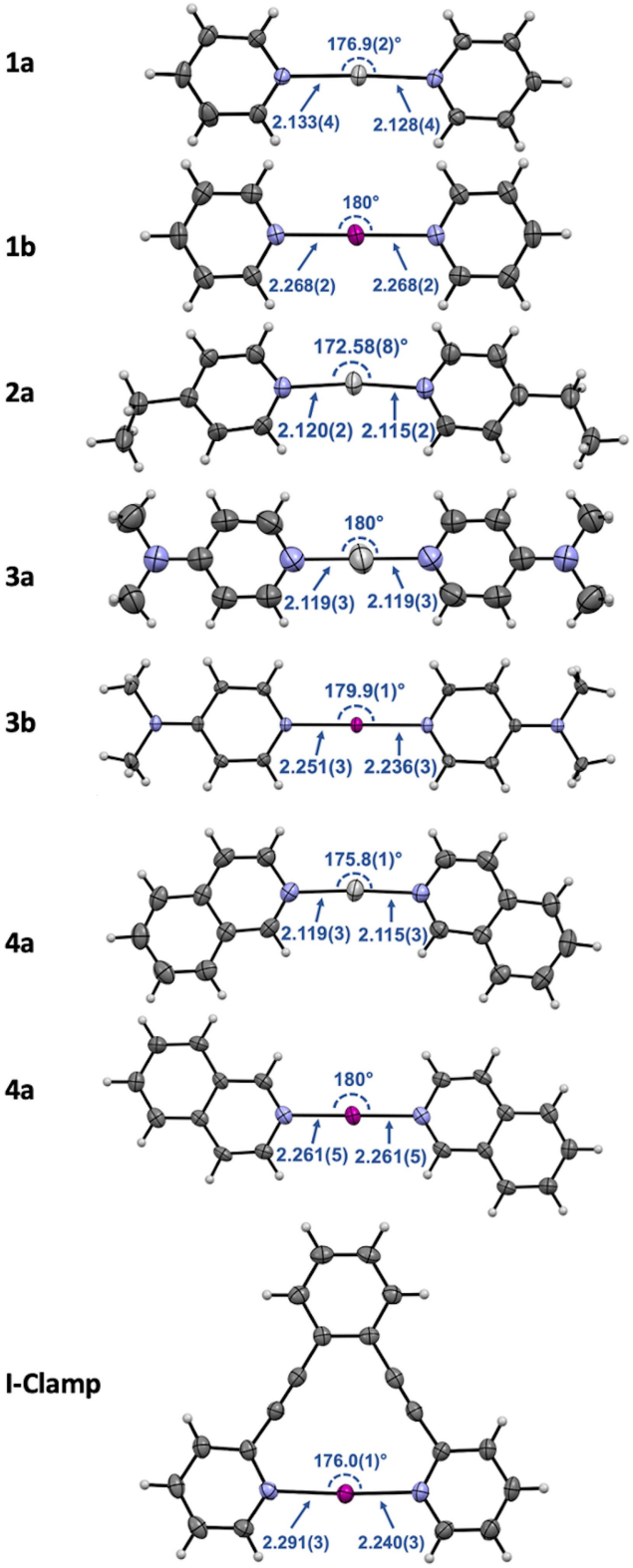

Figure 4. The X-ray structures of **1 a** (*NEVRIQ*), **1 b** (*CICQIQ*), **2 a** (*SURSUW*), **3 a** (*PIZKUF*), **3 b** (*SURTEH*), **4 a** (*RAKNEA*), **4 b** (*RAKQED*) and **I-clamp** (*DAVROL*) with thermal displacement parameters at 50% probability level.

observed in the solution ^{15}N NMR spectra.[54] The three-center four-electron (3c–4e) $[N–I–N]^+$ halogen bond in these systems is very robust and retains its geometry regardless of the ligands (bases) used. The variations observed in the ^{15}N NMR chemical shifts of the iodine(I) complexes **1 b**–**4 b** reflects solely the changes in the chemical environment of the nitrogen nucleus, and are not related to the packing or bond distances and angles of the $[N–I–N]^+$ 3c–4e system. Previous studies have shown that changing the anion present in the halogen(I) complex has no effect on the halogen bonding in solution.[2] However, the effect of changing the anion on the solid state NMR data is yet to be determined, and therefore only a single counterion (PF_6) was used in all the complexes tested herein. The small differences observed for the silver(I) complexes **1 a**–**4 a** very likely result from the stronger packing interaction of the Ag(I) center with the PF_6^- anions and adjacent complexes (*e.g.*, argentophilic interactions). Each ligand has its characteristic ^{15}N NMR chemical shift, which modulates upon the coordination to the silver(I) or iodine(I) cations, causing coordination shifts from -43 to -50 ppm for the silver(I) complexation in the solid state, paralleling the solution behavior. The coordination to the iodine(I) results in an additional −43 to −45 ppm coordination shift (Table 1). The total coordination shifts in solution and in the solid state are very close to each other, *ca.* −100 ppm from the free ligand.

Conclusion

In conclusion, solid-state NMR spectroscopy has been applied to silver(I) and iodine(I) complexes, and the results have been compared and contrasted to their solution-based counterparts in CD_2Cl_2. The solid-state NMR spectra showed the same coordination shifts as the solution NMR spectra, indicating that the technique can be successfully applied to the field of halogen(I) chemistry. Despite the minor and specific practical limitations of solid-state NMR spectroscopy that were identified based on the results, such as solvation and near ambient temperature melting points, the technique can be generally applied to obtain comparable information as its solution-based counterpart. This study reveals that solid-state NMR spectroscopy has unexplored potential in the field of halogen(I) chemistry, where the future direction of the research is undoubtedly heading toward motifs of increasing complexity and diminishing solubilities, both of which will benefit from avoiding the need to dissolve spectroscopic samples prior to testing.

Acknowledgements

The authors would like to thank Mr Esa Haapaniemi for installation and assistance with the NMR hardware, and gratefully acknowledge the Magnus Ehrnrooth Foundation (J.S.W.), the Academy of Finland (K.R. grant no. 351121), and the University of Jyväskylä, Finland for financial support.

Conflict of Interest

The authors declare no conflict of interest.

Data Availability Statement

The data that support the findings of this study are available from the corresponding author upon reasonable request.

Keywords: solid-state NMR · halogen bond · iodine(I) · Barluenga reagent · cation exchange

[1] G. R. Desiraju, P. S. Ho, L. Kloo, A. C. Legon, R. Marquardt, P. Metrangolo, P. Politzer, G. Resnati, K. Rissanen, *Pure Appl. Chem.* **2013**, *85*, 1711–1713.
[2] M. Bedin, A. Karim, M. Reitti, A.-C. C. Carlsson, F. Topić, M. Cetina, F. Pan, V. Havel, F. Al-Ameri, V. Sindelar, et al., *Chem. Sci.* **2015**, *6*, 3746–3756.
[3] A.-C. C. Carlsson, K. Mehmeti, M. Uhrbom, A. Karim, M. Bedin, R. Puttreddy, R. Kleinmaier, A. A. Neverov, B. Nekoueishahraki, J. Gräfenstein, et al., *J. Am. Chem. Soc.* **2016**, *138*, 9853–9863.
[4] J. S. Ward, A. Frontera, K. Rissanen, *Dalton Trans.* **2021**, *50*, 8297–8301.
[5] C. R. Groom, I. J. Bruno, M. P. Lightfoot, S. C. Ward, *Acta Crystallogr. Sect. B* **2016**, *72*, 171–179.
[6] O. Hassel, H. Hope, *Acta Chem. Scand.* **1961**, *15*, 407–416.
[7] J. A. Creighton, I. Haque, J. L. Wood, *Chem. Commun.* **1966**, 229.
[8] J. A. Creighton, I. Haque, J. L. Wood, *Chem. Commun.* **1966**, 892.
[9] I. Haque, J. L. Wood, *J. Mol. Struct.* **1968**, *2*, 217–238.
[10] J. Barluenga, J. M. González, M. A. Garcia-Martin, P. J. Campos, G. Asensio, *J. Chem. Soc. Chem. Commun.* **1992**, *14*, 1016–1017.
[11] J. Ezquerra, C. Pedregal, C. Lamas, J. Barluenga, M. Pérez, M. A. García-Martín, J. M. González, *J. Org. Chem.* **1996**, *61*, 5804–5812.
[12] G. Espuña, G. Arsequell, G. Valencia, J. Barluenga, M. Pérez, J. M. González, *Chem. Commun.* **2000**, *14*, 1307–1308.
[13] M. H. Kolář, P. Hobza, *Chem. Rev.* **2016**, *116*, 5155–5187.
[14] L. Turunen, U. Warzok, R. Puttreddy, N. K. Beyeh, C. A. Schalley, K. Rissanen, *Angew. Chem. Int. Ed.* **2016**, *55*, 14033–14036; *Angew. Chem.* **2016**, *128*, 14239–14242.
[15] L. Turunen, U. Warzok, C. A. Schalley, K. Rissanen, *Chem* **2017**, *3*, 861–869.
[16] S. Yu, E. Kalenius, A. Frontera, K. Rissanen, *Chem. Commun.* **2021**, *57*, 12464–12467.
[17] M. Kandrnálová, Z. Kokan, V. Havel, M. Nečas, V. Šindelář, *Angew. Chem. Int. Ed.* **2019**, *58*, 18182–18185; *Angew. Chem.* **2019**, *131*, 18350–18353.
[18] A. Vanderkooy, A. K. Gupta, T. Földes, S. Lindblad, A. Orthaber, I. Pápai, M. Erdélyi, *Angew. Chem. Int. Ed.* **2019**, *58*, 9012–9016; *Angew. Chem.* **2019**, *131*, 9110–9114.
[19] G. Gong, S. Lv, J. Han, F. Xie, Q. Li, N. Xia, W. Zeng, Y. Chen, L. Wang, J. Wang, et al., *Angew. Chem. Int. Ed.* **2021**, *60*, 14831–14835; *Angew. Chem.* **2021**, *133*, 14957–14961.
[20] Y. Xu, P. M. J. Szell, V. Kumar, D. L. Bryce, *Coord. Chem. Rev.* **2020**, *411*, 213237.
[21] A. D. Bain, in *Annu. Reports NMR Spectrosc.*, Elsevier, **2008**, pp. 23–48.
[22] N. J. Clayden, *Annu. Rep. NMR Spectrosc.* **1992**, *24*, 1–86.
[23] Y. Xu, S. A. Southern, P. M. J. Szell, D. L. Bryce, *CrystEngComm* **2016**, *18*, 5236–5252.
[24] D. Bryce, *IUCrJ* **2017**, *4*, 350–359.
[25] S. E. Ashbrook, S. Sneddon, *J. Am. Chem. Soc.* **2014**, *136*, 15440–15456.
[26] P. Schanda, M. Ernst, *Prog. Nucl. Magn. Reson. Spectrosc.* **2016**, *96*, 1–46.
[27] J. Viger-Gravel, S. Leclerc, I. Korobkov, D. L. Bryce, *CrystEngComm* **2013**, *15*, 3168–3177.
[28] P. Cerreia Vioglio, L. Catalano, V. Vasylyeva, C. Nervi, M. R. Chierotti, G. Resnati, R. Gobetto, P. Metrangolo, *Chem. A Eur. J.* **2016**, *22*, 16819–16828.
[29] M. T. Messina, P. Metrangolo, W. Panzeri, E. Ragg, G. Resnati, *Tetrahedron Lett.* **1998**, *39*, 9069–9072.
[30] C. M. Widdifield, G. Cavallo, G. A. Facey, T. Pilati, J. Lin, P. Metrangolo, G. Resnati, D. L. Bryce, *Chem. A Eur. J.* **2013**, *19*, 11949–11962.
[31] J. Viger-Gravel, S. Leclerc, I. Korobkov, D. L. Bryce, *J. Am. Chem. Soc.* **2014**, *136*, 6929–6942.
[32] P. M. J. Szell, D. L. Bryce, *J. Phys. Chem. C* **2016**, *120*, 11121–11130.
[33] P. M. J. Szell, S. A. Gabriel, R. D. D. Gill, S. Y. H. Wan, B. Gabidullin, D. L. Bryce, *Acta Crystallogr. Sect. C* **2017**, *73*, 157–167.
[34] S. R. Hartmann, E. L. Hahn, *Phys. Rev.* **1962**, *128*, 2042–2053.
[35] S. Berger, S. Braun, *200 and More NMR Experiments: A Practical Course*, WILEY-VCH, Mörlenbach, **2004**.
[36] R. Marek, A. Lycka, *Curr. Org. Chem.* **2002**, *6*, 35–66.
[37] M. Baldrighi, G. Cavallo, M. R. Chierotti, R. Gobetto, P. Metrangolo, T. Pilati, G. Resnati, G. Terraneo, *Mol. Pharm.* **2013**, *10*, 1760–1772.
[38] J. S. Ward, G. Fiorini, A. Frontera, K. Rissanen, *Chem. Commun.* **2020**, *56*, 8428–8431.
[39] J. S. Ward, *CrystEngComm* **2022**, *24*, 7029–7033.
[40] S. Yu, P. Kumar, J. S. Ward, A. Frontera, K. Rissanen, *Chem* **2021**, *7*, 948–958.
[41] J. S. Ward, A. Frontera, K. Rissanen, *Inorg. Chem.* **2021**, *60*, 5383–5390.
[42] S. Wilcox, D. Sethio, J. S. Ward, A. Frontera, R. Lindh, K. Rissanen, M. Erdélyi, *Chem. Commun.* **2022**, *58*, 4977–4980.
[43] D. von der Heiden, K. Rissanen, M. Erdélyi, *Chem. Commun.* **2020**, *56*, 14431–14434.
[44] T. Okitsu, S. Yumitate, K. Sato, Y. In, A. Wada, *Chem. A Eur. J.* **2013**, *19*, 4992–4996.
[45] E. Taipale, M. Siepmann, K.-N. Truong, K. Rissanen, *Chem. A Eur. J.* **2021**, *27*, 17412–17419.
[46] Agilent Technologies Ltd, **2014**, CrysAlisPro.
[47] G. M. Sheldrick, *Acta Crystallogr. Sect. A Found. Adv.* **2015**, *71*, 3–8.
[48] O. V. Dolomanov, L. J. Bourhis, R. J. Gildea, J. A. K. Howard, H. Puschmann, *J. Appl. Crystallogr.* **2009**, *42*, 339–341.
[49] G. M. Sheldrick, *Acta Crystallogr. Sect. C, Struct. Chem.* **2015**, *71*, 3–8.
[50] S. Yu, J. S. Ward, K.-N. Truong, K. Rissanen, *Angew. Chem. Int. Ed.* **2021**, *60*, 20739–20743, *Angew. Chem.* **2021**, *133*, 20907–20911.
[51] E. Kramer, S. Yu, J. S. Ward, K. Rissanen, *Dalton Trans.* **2021**, *50*, 14990–14993.
[52] J. S. Ward, J. Martõnova, L. M. E. Wilson, E. Kramer, R. Aav, K. Rissanen, *Dalton Trans.* **2022**, *51*, 14646–14653.
[53] A. E. Visser, J. G. Huddleston, J. D. Holbrey, W. M. Reichert, R. P. Swatloski, R. D. Rogers, in *Ion. Liq. IV*, American Chemical Society, **2007**, pp. 25–362.
[54] A.-C. C. Carlsson, J. Gräfenstein, A. Budnjo, J. L. Laurila, J. Bergquist, A. Karim, R. Kleinmaier, U. Brath, M. Erdélyi, *J. Am. Chem. Soc.* **2012**, *134*, 5706–5715.
[55] S. Yu, K.-N. Truong, M. Siepmann, A. Siiri, C. Schumacher, J. S. Ward, K. Rissanen, *Cryst. Growth Des.* **2023**, DOI: 10.1021/acs.cgd.2c01162.

Manuscript received: November 29, 2022
Revised manuscript received: January 26, 2023
Accepted manuscript online: February 3, 2023
Version of record online: February 6, 2023